

Gravitino Dark Matter and the Cosmic Lithium Abundances

Sean Bailly, Karsten Jedamzik, Gilbert Moulta

*Laboratoire de Physique Théorique et Astroparticules, UMR5207-CNRS,
Université Montpellier II, F-34095 Montpellier, France.*

Supersymmetric extensions of the standard model of particle physics assuming the gravitino to be the lightest supersymmetric particle (LSP), and with the next-to-LSP decaying to the gravitino during Big Bang nucleosynthesis, are analyzed. Particular emphasis is laid on their potential to solve the “ ${}^7\text{Li}$ problem”, an apparent factor 2–4 overproduction of ${}^7\text{Li}$ in standard Big Bang nucleosynthesis (BBN), their production of cosmologically important amounts of ${}^6\text{Li}$, as well as the resulting gravitino dark matter densities in these models. The study includes several improvements compared to prior studies concerning NLSP hadronic branching ratios, NLSP dark matter densities, the evaluation of hadronic NLSP decays on BBN, BBN catalytic effects, as well as updated nuclear reaction rates. Heavy gravitinos in the constrained minimal supersymmetric standard model (CMSSM) are reanalyzed, whereas light gravitinos in gauge-mediated supersymmetry breaking scenarios (GMSB) are studied for the first time. It is confirmed that decays of NLSP staus to heavy gravitinos, while producing all the dark matter, may at the same time resolve the ${}^7\text{Li}$ problem. For NLSP decay times $\approx 10^3\text{sec}$, such scenarios also lead to cosmologically important ${}^6\text{Li}$ (and possibly ${}^9\text{Be}$) abundances. However, as such scenarios require heavy $\gtrsim 1\text{TeV}$ staus they are likely not testable at the LHC. It is found that decays of NLSP staus to light gravitinos may lead to significant ${}^6\text{Li}$ (and ${}^9\text{Be}$) abundances, whereas NLSP neutralinos decaying into light gravitinos may solve the ${}^7\text{Li}$ problem. Though both scenarios are testable at the LHC they may not lead to the production of the bulk of the dark matter. A section of the paper outlines particle properties required to significantly reduce the ${}^7\text{Li}$ abundance, and/or enhance the ${}^6\text{Li}$ (and possibly ${}^9\text{Be}$) abundances, by the decay of an arbitrary relic particle.

I. INTRODUCTION

Supersymmetry is probably the best studied extension of the standard model (SM) of particle physics. Softly broken supersymmetry seems attractive as it not only may solve the hierarchy problem but also lead to gauge coupling unification at the GUT scale and electroweak symmetry breaking by radiative corrections. Additionally, supersymmetry predicts the existence of new particles whose lightest (LSP), if stable due to some R-parity, may be naturally produced in the right abundance to provide the cosmological dark matter. Here the case of neutralino LSPs has been widely discussed over at least one-and-half decades, whereas the case of gravitino LSPs has received the same widespread detailed attention only since about five years [1, 2, 3, 4, 5, 6, 7, 8, 9, 10, 11, 12, 13, 14, 15, 16]. Gravitino dark matter is special due to its superweak interactions with ordinary matter. It may be produced at fairly high temperatures $10^5 - 10^8\text{GeV}$ during reheating after inflation and, in case it is the LSP, by the decay of the next-to-lightest supersymmetric particle (NLSP) to its SM partner and a gravitino. Due to the gravitationally suppressed interactions of the gravitino the decay with decay time

$$\tau = 48\pi\kappa^{-1} \frac{M_{\text{Pl}}^2 m_{\tilde{G}}^2}{M_{\text{NLSP}}^5} \left(1 - \frac{m_{\tilde{G}}^2}{M_{\text{NLSP}}^2}\right)^{-n} \quad (1)$$

$$\approx 2.4 \times 10^4 \text{sec} \kappa^{-1} \left(\frac{M_{\text{NLSP}}}{300\text{GeV}}\right)^{-5} \left(\frac{m_{\tilde{G}}}{10\text{GeV}}\right)^2$$

typically takes place during or after Big Bang nucleosynthesis (BBN). Here M_{NLSP} and $m_{\tilde{G}}$ are NLSP- and

gravitino- mass, respectively, and M_{Pl} denotes the reduced Planck mass, [17]. Gravitino dark matter is therefore subject to constraint, as it may leave its imprint in the light element abundance yields.

Prediction of the light element abundance yields of ${}^2\text{H}$ (D), ${}^3\text{He}$, ${}^4\text{He}$, and ${}^7\text{Li}$ by an epoch of Big Bang nucleosynthesis is one of the big successes of the hot Big Bang model. It has not only lead to the realization that the Universe has expanded by at least a factor 10^{10} in its past, but also that the bulk of the dark matter must be non-baryonic. In its standard version BBN is reduced to a model of one parameter only, the fractional contribution of the baryonic density to the critical one, $\Omega_b h^2$ (where h is the present Hubble constant in units of $100\text{km s}^{-1}\text{Mpc}^{-1}$). Five years of observations of the cosmic microwave background radiation (CMBR) anisotropies by the WMAP satellite [18] have lead to the comparatively accurate determination of $\Omega_b h^2 \approx 0.02273 \pm 0.00062$ (WMAP-only). This independent estimate of $\Omega_b h^2$ has promoted a comparison of observationally inferred primordial light element abundances with those predicted in standard BBN to an independent cross-check of the cosmic SM. Such a comparison is very favorable for D, broadly consistent yet somewhat inconclusive for ${}^3\text{He}$ and ${}^4\text{He}$, and significantly discrepant for the isotope of ${}^7\text{Li}$. In particular, the primordial ${}^7\text{Li}/\text{H}$ ratio is commonly inferred from ${}^7\text{Li}$ absorption lines in the atmospheres of low-metallicity halo, or globular cluster stars. Most determinations yield ${}^7\text{Li}/\text{H}$ ratios in the range $1 - 2 \times 10^{-10}$ [19, 20, 21, 22, 23], essentially the same value as that determined by the Spite’s 25 years

ago, $\approx 1.12 \pm 0.38 \times 10^{-10}$ as for example,

$${}^7\text{Li}/\text{H} = (1.23^{+0.68}_{-0.32}) \times 10^{-10} \quad (2)$$

[20, 23], or

$${}^7\text{Li}/\text{H} = (1.1 - 1.5) \times 10^{-10}$$

[22]. Some uncertainty remains in the adopted stellar atmospheric temperatures, which may lead to somewhat higher estimates, as in the case of the globular cluster NGC 6397

$${}^7\text{Li}/\text{H} = 2.19 \pm 0.28 \times 10^{-10}$$

[24, 25] or the somewhat controversial result ${}^7\text{Li}/\text{H} = (2.34 \pm 0.32) \times 10^{-10}$ ([26]) for a sample of halo field stars. This is to be compared to the most recent standard BBN prediction of

$${}^7\text{Li}/\text{H} = (5.24^{+0.71}_{-0.67}) \times 10^{-10}$$

[27] taking into account experimental re-evaluations of the for the ${}^7\text{Li}$ abundance most important ${}^3\text{He}(\alpha, \gamma){}^7\text{Be}$ reaction rate [28, 29, 30, 31]. Renewed measurements of this rate has not only increased the central value for ${}^7\text{Li}/\text{H}$ by around 25%, but also reduced its error bar considerably, thereby leaving the discrepancy between prediction and observation more pronounced (around $4.2\text{--}5.3\sigma$ [27]). It is therefore clear that an additional piece to the puzzle is missing.

Whereas it seems essentially ruled out by now that either revised reaction rate data for ${}^3\text{He}(\alpha, \gamma){}^7\text{Be}$ or ${}^7\text{Be}(D, p){}^4\text{He}$ [32] or any other reaction, or a serious underestimate of the stellar atmospheric temperatures (of order 700K), or even a combination of the two effects may resolve the discrepancy, stellar depletion of ${}^7\text{Li}$ stays a viable, and non-exotic, possibility of resolving the primordial ${}^7\text{Li}$ problem. Indeed, atmospheric ${}^7\text{Li}$ may be destroyed by nuclear burning when transported towards the interior of the star. This is also observed in stars with large convective zones, but not in those relatively hotter ($T \sim 6000\text{K}$) radiation dominated main-sequence turn-off stars, which are/were believed, after two decades of research [33], to preserve at least a large fraction of their initial atmospheric ${}^7\text{Li}$. Arguments presented in favor of non-depletion are (a) the essentially uniform observed ${}^7\text{Li}$ abundance over a wide range of different stellar temperatures and metallicities, a pattern which is very difficult to achieve when significant depletion was at work, (b) the absence of star-to-star scatter in ${}^7\text{Li}$ abundances expected to arise when, for example, depletion is induced due to rotational mixing of stars with different rotational velocities, and (c) the claimed presence of relatively large amounts of the much more fragile ${}^6\text{Li}$ isotope in some of those stars (cf. [34] for a review). Thus, taking Occam's razor, many observers believe in the ${}^7\text{Li}$ abundance on the Spite plateau to be the primordial one. Nevertheless, the situation is clearly more complicated, since when gravitational settling ("atomic diffusion") of heavier elements is included, ${}^7\text{Li}$ is predicted to be depleted, albeit

with a pattern which is not observed. In order to reproduce the observations, another turbulent mixing process of unknown nature has to be "fine-tuned" to account for the observed pattern [35, 36]. However, recent observations of the observed patterns in not only ${}^7\text{Li}$, but also Ca and Ti, in the globular cluster NGC 6397, lend indeed some support to this idea, though being currently not statistically overly significant ($2\text{--}3\sigma$). The combination of atomic diffusion and turbulent mixing has thus been claimed to be able to account for a ${}^7\text{Li}$ depletion of factor 1.9 [37], a factor which could go a long way to solve the discrepancy.

In contrast to ${}^7\text{Li}$, standard BBN (SBBN) yields only negligible production of ${}^6\text{Li}/\text{H} \sim 10^{-15} - 10^{-14}$ [38]. This is mainly due to the only ${}^6\text{Li}$ producing reaction in SBBN $D(\alpha, \gamma){}^6\text{Li}$ being a quadrupole transition. ${}^6\text{Li}$ as observed in higher metallicity disk stars and in the Sun is believed to be due to cosmic ray nucleosynthesis, either resulting from spallation reactions $p, \alpha + \text{CNO} \rightarrow \text{LiBeB}$ or cosmic ray fusion reactions $\alpha + \alpha \rightarrow \text{Li}$. Since the time-integrated action of standard supernovae producing cosmic rays is measured by metallicity, it had been a surprise that three groups independently confirmed the existence of ${}^6\text{Li}$ in the atmosphere of the $[Z] \approx -2.2$ low-metallicity star HD84937 (${}^6\text{Li}/{}^7\text{Li} \approx 0.052 \pm 0.019$) [39], a value too high to be comfortably explained by standard cosmic ray nucleosynthesis. The surprise was even bigger when the long-term pioneering observational program of Asplund *et al.* [22] indicated the existence of relatively uniform ${}^6\text{Li}/{}^7\text{Li}$ ratios ~ 0.05 in about ten low-metallicity stars, reminiscent of a primordial plateau (metallicity-independent). Nevertheless, the situation is currently unclear. The presence of ${}^6\text{Li}$ in these hot stars has to be inferred by a minute asymmetry in the atmospheric absorption profile due to the blend of both, the ${}^6\text{Li}$ and ${}^7\text{Li}$ isotopes. Any individual claimed ${}^6\text{Li}$ detection is therefore only at the $2 - 4\sigma$ statistical significance level. Based on observations (of a star which originally, however, was *not* claimed to have ${}^6\text{Li}$) and complete hydrodynamic 3D non-equilibrium simulations of stellar atmospheres, Cayrel *et al.* [40] have recently asserted that line asymmetries due to convective motions in the atmospheres could be easily misinterpreted as atmospheric ${}^6\text{Li}$, and that the claimed abundances are therefore spurious. In contrast, Asplund *et al.* [22] would even infer higher ${}^6\text{Li}/{}^7\text{Li}$ ratios, if they were to utilise their own 3D hydrodynamic non-local thermal equilibrium simulations of line profiles. Further analysis is clearly required.

Concerning cosmic ray production of a putative ${}^6\text{Li}/\text{H} \approx 5 \times 10^{-12}$, a cosmic ray energy of 100eV per interstellar nucleon is required, whereas standard supernovae generated cosmic rays may provide only 5 eV per nucleon at such low metallicities $[Z] \approx -2.75$ (of the star LP 815-43)[41]. Such a ${}^6\text{Li}$ abundance requires therefore a very non-standard early cosmic ray burst, preferentially acting at higher redshift [42], possibly connected to radio-loud quasars and the excess entropy in clusters of galaxies [43], or to a significant fraction of baryons entering very

massive black holes [41]. The requirements are extreme and no compelling candidate has been identified. Alternatively, it may be that the ${}^6\text{Li}$ is produced in situ, due to fusion reactions in solar flares [44].

The anomaly in the ${}^7\text{Li}$ abundance and/or the purported one in the ${}^6\text{Li}$ abundance, could also be due to physics operating immediately during or shortly after the BBN epoch, possibly connected to the dark matter. It has been long known that ${}^6\text{Li}$ is easily produced in abundance in non-thermal ${}^3\text{H}(\alpha, n){}^6\text{Li}$ and ${}^3\text{He}(\alpha, p){}^6\text{Li}$ reactions during and after BBN without much disturbing the other light elements. Here energetic ${}^3\text{H}$ and ${}^3\text{He}$ may be produced by ${}^4\text{He}$ spallation- or photodisintegration- processes induced by the decay of relic particles [45, 46, 47, 48] or residual annihilation of dark matter particles [49]. A $m_\chi \approx 10\text{ GeV}$ neutralino of the WMAP density, and with substantial hadronic s-wave annihilation, as sometimes invoked to explain the DAMA/Libra anomaly [50], would, for example, synthesize a ${}^6\text{Li}$ abundance well in excess of that in HD84937. Similarly, the ${}^7\text{Li}$ abundance may be also affected by particle decay (but less by annihilation). Early attempts to explain the ${}^7\text{Li}$ anomaly by ${}^7\text{Li}$ photodisintegration induced by the electromagnetic decay of a NLSP to a gravitino at $\tau \sim 10^6\text{sec}$ [2], were subsequently shown to be in disaccord with either, a reasonable lower limit on the D/H ratio or an upper limit on the ${}^3\text{He}/\text{D}$ ratio [51]. However, it was shown that the injection of extra neutrons between the mid and end $\sim 100 - 3000\text{sec}$ of the BBN epoch can affect a substantial reduction of the final ${}^7\text{Li}$ abundance [47]. Moreover, if these neutrons are injected energetically, as is the case during the decay of a weak-scale mass particle, their ${}^4\text{He}$ spallation may at the same time be the source of an appreciable ${}^6\text{Li}$ abundance.

This led to the realization that $m_{\tilde{\tau}} \approx 1\text{ TeV}$ supersymmetric staus decaying into $m_{\tilde{G}} \approx 100\text{ GeV}$ gravitinos during BBN may resolve two lithium problems at once [47]. Subsequent more detailed calculations of stau freeze-out abundances, life times, and hadronic branching ratios within the constrained minimal supersymmetric standard model (CMSSM) [52] and [53] confirmed these findings (cf. also to Ref. [54] and [55]).

The present paper presents a re-/extended analysis of supersymmetric (SUSY) scenarios with gravitino LSP's which may solve one, or both, lithium anomalies. The reasons for such a reanalysis are multifold.

1. Reference [52] as well as [53] analyzed scenarios only for large, electroweak scale gravitino masses. The present paper studies the case of light $\sim 10\text{ MeV}-1\text{ GeV}$ gravitinos as well. Light gravitinos are typically emerging in gauge-mediated SUSY breaking scenarios (GMSB). A consistent analysis of GMSB scenarios is performed. Finally, for heavier electroweak scale gravitino masses, as predicted in the CMSSM, an improved scan of gravitino masses is presented.

2. The adopted hadronic branching ratios in [52] (based on Ref. [4]) are somewhat rough approximations

only. For example, as shown in [12], the hadronic branching ratio for the decay of the lighter stau, $\tilde{\tau}_1 \rightarrow \tilde{G}\tau q\bar{q}$, is larger when production of $q\bar{q}$ pairs by intermediate virtual photons, and not only Z-bosons, is taken into account as well.

3. The $q\bar{q}$'s have been noted to be injected at much lower energy [12] than taken in the approximative treatment of [52]. In particular, it has been argued that for accurate BBN calculations the effective energy ϵ_{HAD} should be taken as the mean in the $q\bar{q}$ invariant mass $m_{q\bar{q}}$.

4. It will be shown in Section II, that taking the mean invariant mass $m_{q\bar{q}}$ as proposed in [12] represents an approximation as well. Indeed, a fully proper calculation requires knowledge of the energy spectrum of the injected nucleons.

5. It has been recently pointed out that charged electroweak mass scale particles, such as the $\tilde{\tau}$, when present during the BBN epoch, may lead to interesting catalytic effects [56, 57, 58]. In particular, catalytic enhancement of ${}^6\text{Li}$ production [56, 59] has an important effect for stau life times $\tau_x \gtrsim 3000\text{sec}$, whereas catalytic enhancement of ${}^7\text{Li}$ destruction [60] is less important for stau NLSPs. The impact of both effects on the $\tau_x \approx 10^3\text{sec}$ lithium-solving parameter space has already been investigated in Ref. [61] (see also [62, 63] for other papers on catalysis). The present paper takes full account of the proposed catalytic processes.

6. Similarly, Pospelov [64, 65] has made the interesting suggestion that ${}^9\text{Be}$ may be produced due to catalytic effects. These effects are included in the present study and their significance is addressed.

7. Finally, the re-evaluation of the main ${}^7\text{Li}$ producing rate [27, 28, 29, 30, 31], as well as a shift in $\Omega_b h^2$ [18], as indicated in the introduction, has increased the predicted standard BBN ${}^7\text{Li}$ abundance. These changes are included in the present paper as well as recent changes in some catalytic reactions rates [66].

II. DEPENDENCE OF RESULTS ON NUCLEON SPECTRUM

In [12] it was argued that the quantity

$$\langle m_{q\bar{q}} \rangle = \frac{1}{\Gamma_{\text{tot}}(\tilde{\tau})} \int_{m_{q\bar{q}}^{\text{cut}}}^{m_{\tilde{\tau}} - m_{\tilde{G}} - m_{\tau}} dm_{q\bar{q}} m_{q\bar{q}} \frac{d\Gamma(\tilde{\tau} \rightarrow \tau \tilde{G} q\bar{q})}{dm_{q\bar{q}}} \quad (3)$$

should be taken as the “effective hadronic energy” $E_{\text{Had}}(\tilde{\tau} \rightarrow \tau \tilde{G} q\bar{q})$ for the computation of BBN yields with decaying particles. It was noted that this is considerably lower for hadronic decays of $\sim\text{TeV}$ stau's than the adopted $(m_{\tilde{\tau}} - m_{\tilde{G}})/3$ in [52]. Though this is a good comment, the situation is much more complicated. In contrast to electromagnetic decays, there is *no* obvious sensible definition of an “effective hadronic energy”. For

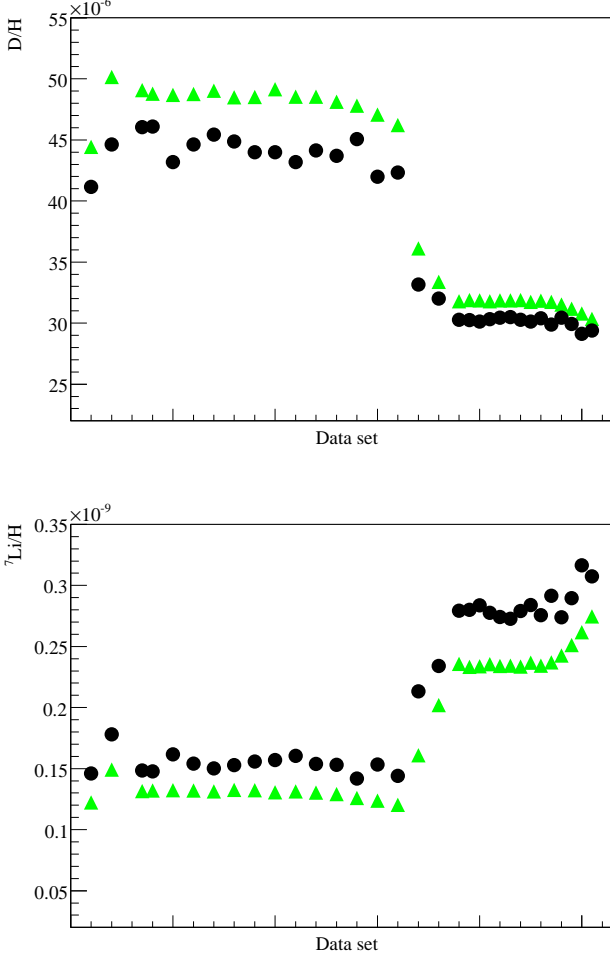


FIG. 1: D/H (upper) and ${}^7\text{Li}/\text{H}$ (lower) abundances computed for a number of selected models with $m_{\tilde{\tau}} \approx 1 \text{ TeV}$ and $\Omega_{\tilde{G}} h^2 \approx 0.1$ (see text for further detail) when (a) the invariant mass approximation is used (green triangles) and (b) the analysis is performed using a realistic nucleon energy spectrum (black dots). The left (right) plateau show models with approximate decay times $\tau \approx 10^3 \text{ sec}$ ($\tau \approx 300 - 600 \text{ sec}$), respectively. They correspond to models in the blue (red) regions of Fig. 5, respectively.

example, ten $q\bar{q}$ fluxtubes of $E_{CM} = 100 \text{ GeV}$ produce about 13.5 neutrons and protons (of varying energy), whereas one fluxtube of $E_{CM} = 1 \text{ TeV}$ produces only 3.2 nucleons. Similarly, the injection of ten 10 GeV neutrons at temperature $T = 30 \text{ keV}$ lead to the production of 4.3 thermalized D, 14.4 neutrons, and 4.0 nucleon number $A = 3$ -nuclei. This needs to be compared to 0.5 D, 1.45 neutrons and 0.7 $A = 3$ -nuclei for one injected 100 GeV neutron. In both examples one started with the same initial “hadronic energy”, with the result being vastly different. The number ΔN_i^{casc} (neutrons, D, ${}^3\text{H}$, ${}^6\text{Li}$, ...) of thermalized nucleons/nuclei i produced per X particle decay at temperature T may be written in the following

form

$$\Delta N_i^{casc} = B_h \sum_{j=p,n} \int dE_j P_j^{had}(E_j) \frac{dN_i^{casc}}{dN_j}(E_j, T) \quad (4)$$

where $P_j^{had}(E_j) = (dN_j/dE_j)$ is the distribution function of nucleons j (protons, neutrons) with initial energy E_j injected into the plasma by the X decay, normalized such that

$$\int dE_j P_j^{had}(E_j) = \langle N_j \rangle \quad (5)$$

gives the mean number of injected nucleons j per hadronic decay. In the above the quantity $dN_i^{casc}/dN_j(E_j, T)$ gives the produced (and thermalized) nucleons/nuclei i per injected nucleon j injected at initial energy E_j , and B_h is the hadronic branching ratio. For the computation of ΔN_i^{casc} a detailed analysis of the thermalisation of an injected nucleon j , as well as the thermalisation of all produced secondary (and higher) generations of non-thermal nucleons and nuclei due to energetic nucleon inelastic- and spallation- scattering processes on thermal nucleons and nuclei is required (cf. [67]).

The invariant mass $m_{q\bar{q}}$ gives the energy E_{CM} of the $q\bar{q}$ fluxtube in the $q\bar{q}$ center-of-mass reference system. This quantity does *not*, however, give the energy of the fluxtube in the cosmic rest frame (stau rest frame). The latter is much larger. Nevertheless, approximating $P_j^{had}(E_j)$ by the nucleon energy distribution in the center-of-mass frame of $q\bar{q}$, resulting after fragmentation of a $q\bar{q}$ fluxtube of energy $\langle m_{q\bar{q}} \rangle$, is still somewhat useful, since in certain temperature ranges, such as $50 \text{ keV} \lesssim T \lesssim 80 \text{ keV}$, the BBN yields mostly only depend on the number of nucleons injected, as long as they are somewhat energetic $E_{kin} \gtrsim 1 \text{ GeV}$. Whereas the energy of the created nucleons is not an invariant of the reference system, the number is. However, even this corresponds to an approximation.

For a limited number of scenarios we have computed a realistic nucleon spectrum. This spectrum was then used as input to perform accurate BBN calculations. The scenarios studied are $\sim 1 \text{ TeV}$ staus decaying between $\tau \approx 300 - 1200 \text{ sec}$ into gravitinos, with the decay producing $\Omega h^2 \approx 0.1$ in gravitinos. Fig. 1 shows the yields of D/H and ${}^7\text{Li}/\text{H}$ as obtained either from the realistic nucleon spectrum or from the approximation of a nucleon distribution resulting from a $q\bar{q}$ pair of energy $\langle m_{q\bar{q}} \rangle$ in its center-of-mass frame. It is seen that the realistic spectrum gives larger ${}^7\text{Li}$ and lower Deuterium abundances by $\lesssim 10 - 15\%$ as compared to the $\langle m_{q\bar{q}} \rangle$ approximation. It is cautioned however, that the relative error is only small for comparatively early decays. In what follows, when not stated explicitly otherwise, all figures shown employ this approximation.

All BBN calculations assume $\Omega_b h^2 = 0.02273$ and employ the recent reevaluation of the ${}^3\text{He}(\alpha, \gamma){}^7\text{Be}$ rate by [27]. For details concerning the BBN calculations the

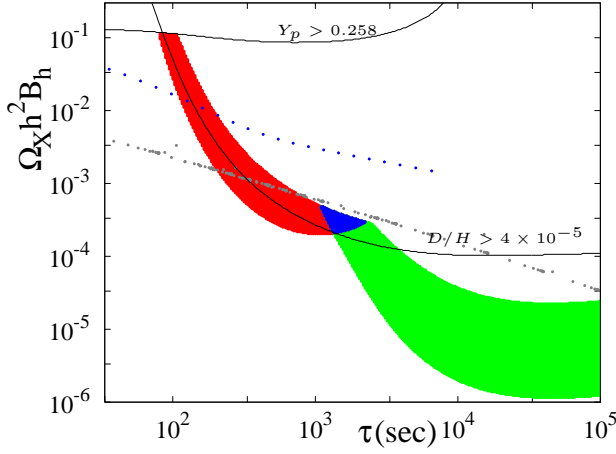


FIG. 2: Parameter space in the $\Omega_X h^2 B_h$ versus τ plane where decaying relic neutral particles have impact on the ^7Li and ^6Li abundancies following Ref. [47]. Here Ω_X is the fractional contribution to the critical density the decaying particle would have today if it wouldn't have decayed, h is the Hubble constant in units of $100\text{kms}^{-1}\text{Mpc}^{-1}$, B_h is the hadronic branching ratio, and τ is the particle life time. The color coding of the areas is as follows: (red) $^7\text{Li}/\text{H} < 2.5 \times 10^{-10}$; (green) $0.015 < ^6\text{Li}/^7\text{Li} < 0.3$; and (blue) both $^7\text{Li}/\text{H} < 2.5 \times 10^{-10}$ and $0.015 < ^6\text{Li}/^7\text{Li} < 0.3$. Other (relevant) constraints on light elements are taken to be $D/\text{H} < 5.3 \times 10^{-5}$ and the helium mass fraction $Y_p < 0.258$, as indicated by a line. The black solid line labeled $D/\text{H} > 4 \times 10^{-5}$ shows how lithium-friendly parameter space is reduced when a less conservative limit on D/H is applied. The figure also shows by the grey and blue points, following essentially lines, the prediction for stau-NLSPs in the CMSSM assuming a gravitino mass of $m_{\tilde{G}} = 50\text{ GeV}$ and the prediction for neutralino NLSPs in a GMSB scenario assuming a gravitino mass of $m_{\tilde{G}} = 100\text{ MeV}$, respectively. To produce this figure, the hadronic decay of a 1 TeV particle into a quark-antiquark pair has been assumed. Results for other initial states and particle masses M_X may vary by a factor of a few such that the figure should be interpreted as indicative only.

reader is referred to [67] (and [61]). Catalytic rates are taken from the recent papers [59] and [66]. Details relevant to the CMSSM and GMSB supersymmetric models, NLSP freeze-out abundances, as well as the calculation of hadronic branching ratios will be presented elsewhere. This analysis was performed using several public numerical codes: SuSpect [68] (a supersymmetric particle spectrum calculator), micrOMEGAs [69] (a dark matter relic density calculator), CalcHEP [70] (an automatic matrix element generator), and PYTHIA [71] (a Monte-Carlo high-energy-physics event generator).

III. A GUIDE TO THE MODEL BUILDER

In this section we discuss, in a generic way, the relic decaying particle parameter space that is interesting for the ^7Li , ^6Li (and ^9Be) abundances. The discussion will then prove useful in the following sections for the identifica-

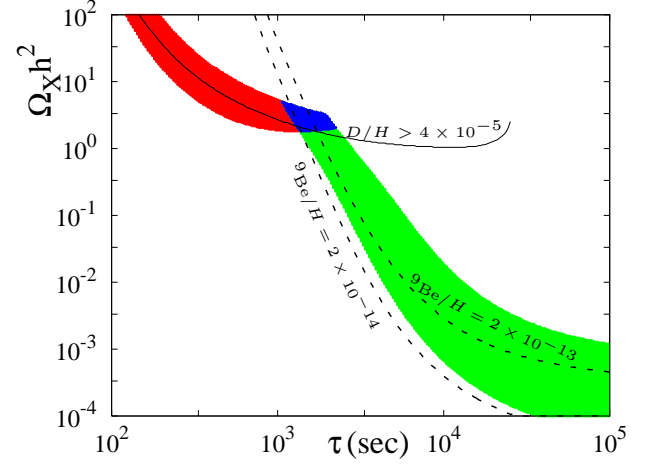


FIG. 3: Parameter space in the $\Omega_X h^2$ - τ_X plane where *charged* relic decaying particles have impact on the cosmic ^7Li , ^6Li , and (possibly) ^9Be abundances without violating other light-element constraints. Here $M_X = 1\text{ TeV}$, $B_h = 10^{-4}$ and hadronic primaries of 1 TeV $q\bar{q}$ fluxtubes have been assumed. The color code is as described in caption Fig. 2. The two dashed lines delimit the band $2 \times 10^{-14} \lesssim ^9\text{Be}/\text{H} \lesssim 2 \times 10^{-13}$, whereas the solid line indicates $D/\text{H} = 4 \times 10^{-5}$.

tion of scenarios in our particular model, supersymmetry with gravitino LSPs. Fig.2 shows the parameter space in relic decaying particle abundance, hadronic branching ratio B_h , and X -particle decay time which has impact on the cosmic lithium abundances while respecting all other abundance constraints. Note that results are only dependent on the product of $\Omega_X h^2 B_h$, where Ω_X is the fractional contribution of the X -particle to the present critical density, if it wouldn't have decayed. (The Ω_X may be converted to the X -particle number to entropy density n_X/s via $n_X M_X/s = 3.6639 \times 10^{-9} \text{ GeV} \Omega_X h^2$, where M_X is the X -particle mass.) Evidently the results depend as well on the hadronic branching ratio of the X -particle decays. To produce the plots in Figs.2 and 3 we made the assumption of hadronic decays described by a $M_X = 1\text{ TeV}$ X -particle decaying into a $q\bar{q}$ pair occurring with probability B_h . This does not correspond exactly to the situation of NLSPs decays into gravitinos \tilde{G} , i.e. neutralino $\chi \rightarrow \tilde{G}q\bar{q}$ and stau $\tilde{\tau} \rightarrow \tilde{G}\tau q\bar{q}$, such that, for our analysis, the figures should be used only as guides. However, making different assumptions for particle mass and initial (hadronic) post-decay state make in many cases only changes of factors of order 2 – 3.

It is seen that for early decay times within a "banana"-shaped region the ^7Li abundance may be significantly reduced ($^7\text{Li}/\text{H} < 2.5 \times 10^{-10}$ red area). Here the upper envelope of the area is defined by the constraint $D/\text{H} \lesssim 5.3 \times 10^{-5}$ and the lower envelope by $^7\text{Li}/\text{H} \gtrsim 2.5 \times 10^{-10}$. A value of $D/\text{H} = 5.3 \times 10^{-5}$ may be already uncomfortably large. Therefore, the accordingly labeled solid line in Fig.2 indicates the less conservative $D/\text{H} < 4.0 \times 10^{-5}$ limit. The green area indicates the region where a $^6\text{Li}/^7\text{Li}$ ratio of $0.015 \lesssim ^6\text{Li}/^7\text{Li} \lesssim 0.3$ has

been synthesized. Here the upper end of the range requires already some post BBN stellar ${}^6\text{Li}$ depletion (relative to ${}^7\text{Li}$). The figure illustrates that for $\tau_X \gtrsim 10^3$ sec there exists plenty of parameter space which may produce an observationally important ${}^6\text{Li}$ abundance by hadronic particle decays. Moreover, as advocated in Ref. [47], a region around $\tau_X \approx 1000$ sec and $\Omega_X h^2 B_h \approx 2 \times 10^{-4}$ may resolve both lithium anomalies at once.

In Fig. 2 it has been implicitly assumed that the decaying particle is neutral. In case it is charged, catalytic effects may have a strong impact on the ${}^6\text{Li}$ abundance [56], particularly for small B_h . Moreover, catalytic effects may also lead to the production of ${}^9\text{Be}$ [64], though it is currently not clear if this indeed happens (cf. [66]). Note that ${}^9\text{Be}$ production is impossible with hadronic effects only. Fig. 3 shows the ${}^7\text{Li}$, ${}^6\text{Li}$, and (possibly) ${}^9\text{Be}$ friendly areas for a charged massive particle decaying during the BBN era. Here a hadronic branching ratio $B_h = 10^{-4}$ and particle mass $M_X = 1$ TeV have been assumed. In order to compute ${}^9\text{Be}/\text{H}$ ratios we follow the assumptions in Ref. [64], keeping in mind the possibility of very significant modifications [66]. It is noted that in Fig. 2 an ordinate $\Omega_X h^2 B_h$ has been chosen, whereas in Fig. 3 the ordinate $\Omega_X h^2$ is shown for one particular choice of B_h [72]. It is intriguing to remark that when the decaying particle is charged, not only may the ${}^7\text{Li}$ and ${}^6\text{Li}$ anomalies be solved, but for the same parameters an observationally important $2 \times 10^{-14} \lesssim {}^9\text{Be} \lesssim 2 \times 10^{-13}$ abundance [73] may be synthesized as well. This is seen by the dashed lines in Fig. 3 passing through the doubly preferred region at $\Omega_X h^2 B_h \approx 3 \times 10^{-4}$ and $\tau_X \approx 1500$ sec.

Though the results of this section are essentially generic, and may be used as guide lines for constructing other particular “lithium-friendly” decaying particle scenarios, Fig. 2 also shows predictions within two particular setups in supersymmetric extensions of the standard model. The sequence of grey points gives the prediction of stau-NLSPs in the CMSSM under the assumption of a gravitino mass of $m_{\tilde{G}} = 50$ GeV. Such scenarios come very close to the doubly-preferred blue region at $\tau_X \approx 1000$ sec, which illustrates that (within the approximations) the ${}^6\text{Li}$ and ${}^7\text{Li}$ observed abundances could be modified in an observationally favored way by stau decay, albeit for a stau mass $m_{\tilde{\tau}} \sim 1$ TeV inaccessible to the LHC. This scenario will be analyzed once more in Section IV. It is noted here that though it seems somewhat inconsistent to show $\tilde{\tau}$ NLSP decay in Fig. 2, due to catalytic effects which are not taken into account in that figure, conclusions concerning the ${}^7\text{Li}$ and ${}^6\text{Li}$ preferred regions are hardly modified when catalytic effects are included (aside from ${}^9\text{Be}$). The sequence of blue points gives the prediction of neutralino NLSPs in a GMSB model assuming $m_{\tilde{G}} = 100$ MeV. Such NLSPs, characterized by fairly large freeze-out densities and hadronic branching ratios, though they would produce too much ${}^6\text{Li}$ when decaying late, could solve the ${}^7\text{Li}$ problem for decay times $\tau_X \sim 100 - 400$ sec. This possibility is studied in detail in Section V.

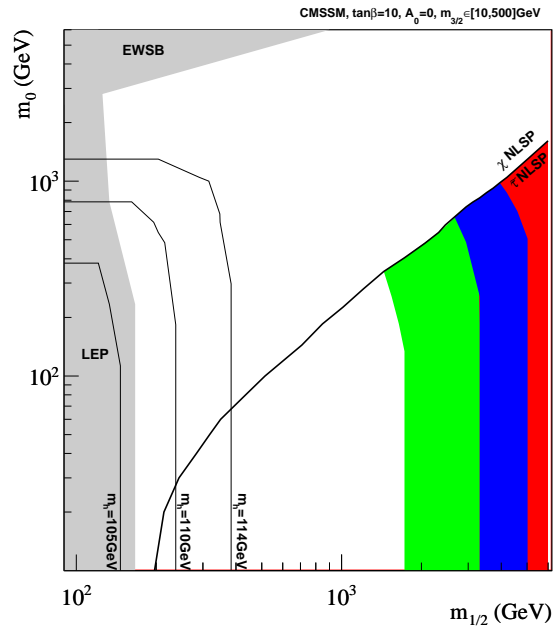


FIG. 4: Parameter space in the CMSSM $m_0 - m_{1/2}$ plane where NLSP decay during BBN results in observationally favored modifications of the ${}^7\text{Li}$ and/or ${}^6\text{Li}$ abundances with respect to standard BBN. Here $\tan\beta = 10$ has been assumed. The color coding indicate: (red) ${}^7\text{Li}/\text{H} < 2.5 \times 10^{-10}$, (green) $0.015 < {}^6\text{Li}/{}^7\text{Li} < 0.15$, and (blue) ${}^7\text{Li}/\text{H} < 2.5 \times 10^{-10}$ and $0.015 < {}^6\text{Li}/{}^7\text{Li} < 0.66$. Other constraints are as in Fig. 2. White areas are ruled out by BBN. The area labeled “LEP” is excluded by LEP accelerator constraints, whereas the area labeled “EWSB” does not lead to electroweak symmetry breaking. The line labeled “ χ NLSP” and “ $\tilde{\tau}$ NLSP” delineates the parameter space where a neutralino χ is the NLSP from that where the stau $\tilde{\tau}$ is the NLSP. The three lines on the left hand side give contours for the lightest neutral Higgs mass, as labeled.

IV. LITHIUM AND HEAVY LSP GRAVITINOS

Weak scale mass “heavy” gravitinos are generally expected in the constrained minimal supersymmetric model (CMSSM), which will be utilised for the present analysis with the gravitino mass, $m_{\tilde{G}} > 10$ GeV taken as a free parameter. Other parameters in the CMSSM are: m_0 , $m_{1/2}$ – at the GUT-scale unified scalar, fermionic (gaugino) soft supersymmetry breaking masses, respectively, A_0 – trilinear couplings in the scalar sector (assumed to be zero throughout), and $\tan\beta$ – the ratio of the vacuum expectation values of the two Higgs required in supersymmetry. It is known that the CMSSM with weak-scale LSP gravitinos may lead to cosmologically interesting changes in the primordial ${}^6\text{Li}$ and ${}^7\text{Li}$ abundances when the superpartner to the tau lepton, the stau, is the NLSP [47, 52, 74]. This may be seen given their abundances, which can be approximated for moderate $\tan\beta$

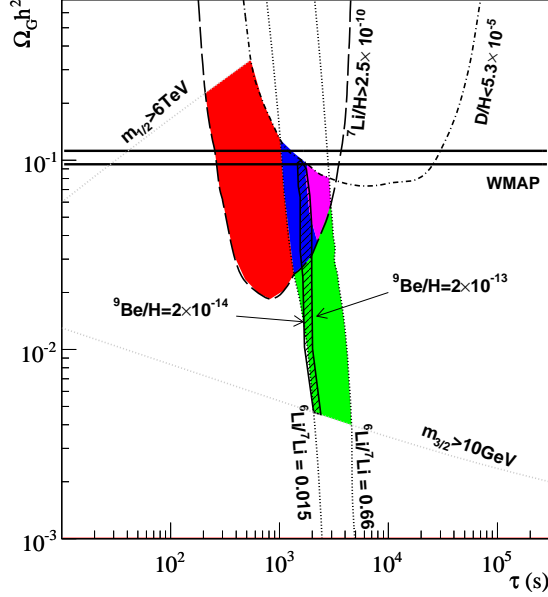


FIG. 5: Gravitino relic density $\Omega_{\tilde{G}} h^2$ versus NLSP (stau) life time τ corresponding to the CMSSM models studied in Fig. 4. Color coding is as in Fig. 4 except that “pink” shows regions where $^7\text{Li}/\text{H} < 2.5 \times 10^{-10}$ and $0.15 < ^6\text{Li}/^7\text{Li} < 0.66$ accounting for the possibility of ^6Li depletion. The cross-hatched region shows parameter space where $2 \times 10^{-14} < ^9\text{Be}/\text{H} < 2 \times 10^{-13}$, though the estimate is uncertain. Other lines show (as labeled) light element abundance constraints, the scan range in $m_{1/2}$ and $m_{\tilde{G}}$, as well as the by WMAP inferred range for the dark matter density.

by [75]

$$\Omega_{\tilde{\tau}} h^2 \approx (2.2 - 4.4) \times 10^{-1} \left(\frac{m_{\tilde{\tau}_1}}{1\text{TeV}} \right)^2, \quad (6)$$

their typical hadronic branching ratios $B_h \approx 10^{-4} - 10^{-2}$, and life times in the range $\tau_{\tilde{\tau}} \approx 10^2 - 10^5 \text{sec}$ as controlled by Eq.(2) with $\kappa = 1, n = 4$. Note that the range in the approximation Eq.(6) takes into account possible co-annihilation with the other sleptons (but does not account for co-annihilation with a neutralino or other specific effects at larger $\tan\beta$, such as mixings, higgs resonances, enhanced couplings, etc.). When compared to Fig. 2 and taking $\tan\beta = 10$, one finds for instance that staus in the mass range $m_{\tilde{\tau}} \approx 1 - 1.5 \text{TeV}$, having $B_h \gtrsim 10^{-3}$ and decaying into gravitinos with $m_{\tilde{G}} \approx 50 - 200 \text{GeV}$ pass right through the preferred (blue) region. A somewhat heavier stau $\approx 2 \text{TeV}$, with a $B_h \approx 2 \times 10^{-3}$ and a $\Omega_{\tilde{\tau}} h^2 B_h \approx 1 \times 10^{-3}$, would be *only* ^7Li friendly as can be seen from Fig. 2, for $m_{\tilde{G}} \approx 100 \text{GeV}$. The lithium friendly parameter space for the CMSSM with $\tan\beta = 10$ is shown in Figs. 4 and 5. The calculations leading to Figs. 4 and 5 include the improvements (1)-(3),(5), and (6) of the list given in the Introduction, but not improvement (4). Treating each case with a realistic

nucleon spectrum is numerically too expansive, and will be only done for a few models below. Note that Figs. 4 and 5 really show results of higher-than-two dimensional parameter space. Even at fixed $\tan\beta$ and A_0 the results in the $m_0 - m_{1/2}$ plane shown in Fig. 4 are for a variety of gravitino masses. In particular, blue areas in the $m_0 - m_{1/2}$ plane are covering up green and red areas which result for different choices of $m_{\tilde{G}}$. The figure, and other figures which follow, thus show where ^6Li (green), ^7Li (red), and ^6Li and ^7Li (blue) friendly regions are expected, *in case* $m_{\tilde{G}}$ has been approximately chosen. In contrast, in white regions for no $m_{\tilde{G}}$ within the adopted range may light element abundance constraints be met.

Figs. 4 and 5 may be directly compared to Figs. 1 and 2 of [52]. It is seen that the doubly preferred (blue) region is narrower in [52] compared to the present study. This is simply due to a finer sampling of the gravitino mass in the present paper. Furthermore, models with larger stau life times, $\tau_{\tilde{\tau}} \gtrsim 5 \times 10^3 \text{sec}$, are due to catalytic ^6Li and (possibly) ^9Be overproduction now ruled out [14, 65]. Finally, it is noted that in the $\Omega_{3/2} h^2 - \tau_{\text{NLSP}}$ plane the doubly preferred (blue) region has hardly moved. This is somewhat surprising since for ~ 2 larger B_h (point 2 in Introduction), as is the case, one would expect for the region to move a factor ~ 2 lower in $\Omega_{\tilde{\tau}} h^2$ (and thus $\Omega_{3/2} h^2$) as to not overproduce D. Nevertheless, this effect is counter-balanced by a lower effective $\langle m_{q\bar{q}} \rangle$ (point 3 in Introduction), implying less “distortion” of the light elements than initially envisioned.

Scenarios where stau NLSPs decay at around $\tau \approx 1000 \text{sec}$ into gravitinos, thereby solving both lithium problems at once, have the added, and totally accidental, benefit of coming tantalizingly close to producing all the dark matter in form of warm gravitinos during the decays. This is nicely illustrated in Fig. 5 where the blue area just overlaps from below with the WMAP strip, and models at higher $\Omega_{3/2} h^2$ are ruled out by Deuterium overproduction, $D/\text{H} > 5.3 \times 10^{-5}$. It is therefore interesting to see if this conclusions survives when a calculation of improved accuracy is performed. The results in Fig. 5 rely on approximating the “hadronic energy” by $\langle m_{q\bar{q}} \rangle$ of Eq.(3). When properly calculating the hadronic energy release employing a realistic energy distribution of the nucleons leads to a milder D overproduction constraint than expected from the $\langle m_{q\bar{q}} \rangle$ approximation as shown in section II, thus pushing the blue area more upwards into the WMAP strip. This is seen in Fig. 1 where results for CMSSM ($\tan\beta = 10$) scenarios with $\Omega_{\tilde{G}} h^2$ close to 0.1 are shown, which have been computed without the $m_{q\bar{q}}$ approximation. Such scenarios are thus *fully consistent* with producing *all* the dark matter non-thermally.

It is of interest if catalytic effects due to the electrically charged staus may also lead to a cosmologically important ^9Be abundance [64, 65] in the doubly preferred parameter space. Indeed, this is the case, as may be seen in Fig. 5 where the $^9\text{Be}/\text{H}$ -ratio in the range $2 \times 10^{-14} \lesssim ^9\text{Be}/\text{H} \lesssim 2 \times 10^{-13}$ is indicated by the cross-hatched region. This is indeed very interesting since

the observed ${}^9\text{Be}/\text{H}$ in the lowest metallicity stars is ${}^9\text{Be}/\text{H} \approx 3 \times 10^{-14} - 10^{-13}$ [73], thus close to the predicted one.

In Table I parameters and BBN yields for some particular SUSY points in the CMSSM (and GMSB, cf. Section V) for $\tan\beta = 10$ are shown. One notes two classes of models, those which synthesize much ${}^6\text{Li}$ (and ${}^9\text{Be}$), for larger τ_χ , and those which significantly reduce ${}^7\text{Li}$ for smaller τ_χ , with the latter models also accounting for the dark matter produced during the decay. In either model D/H may be significantly less than 4×10^{-5} . Models which accomplish both, a factor > 2 destruction of ${}^7\text{Li}$ as well as cosmologically interesting production of ${}^6\text{Li}$ (and possibly ${}^9\text{Be}$), however, typically tend to have $\text{D}/\text{H} > 4 \times 10^{-5}$. Finally, it is noted that even in the presence of hadronic decays, i.e. injection of extra neutrons, the ${}^9\text{Be}/{}^6\text{Li}$ ratio falls typically in the range $1 - 4 \times 10^{-3}$, as proposed in Ref. [64] in the absence of extra neutrons.

Last but not least Fig. 6 shows results for the CMSSM and $\tan\beta = 50$. As was already noted in [52], for $\tan\beta$ large, and a stau NLSP (for neutralino NLSPs cf. Section V), typical $\Omega_{\tilde{\tau}} h^2 B_h(\tilde{\tau}) \lesssim 10^{-4}$ are too small to resolve the ${}^7\text{Li}$ problem (cf. Fig. 2). This is due to the smaller freeze-out abundance due to efficient annihilations of $\tilde{\tau}\tilde{\tau}$ into $W^+W^- (ZZ)$ and hh (light CP- even Higgses) for large $\tan\beta$, as compared to the $\tilde{\tau}\tilde{\tau} \rightarrow \tau\tau$ channel which controls the abundance at low $\tan\beta$. Such effects can be due to Higgs poles or large left-right stau mixing for relatively light stau masses (as shown in [76, 77] in non-CMSSM scenarios). In the CMSSM and for very heavy stau NLSPs as is the case in Fig. 6, W^+W^- plus ZZ channels become dominant. Nevertheless, there remains parameter space which may synthesize observationally important primordial ${}^6\text{Li}$ and ${}^9\text{Be}$ abundances at once. This may occur for staus as light as $m_{\tilde{\tau}} \approx 500\text{GeV}$, potentially visible at the LHC. It is noteworthy that for very heavy $m_{\tilde{\tau}} \gtrsim 2\text{TeV}$ there are again regions where either ${}^7\text{Li}$ alone or both ${}^6\text{Li}$ and ${}^7\text{Li}$ are synthesized at the observationally inferred level. Furthermore, due to the smallness of $\Omega_{\tilde{\tau}} h^2$ for relatively light staus, only a small fraction of the dark matter would be produced by stau decays, with the "missing" gravitinos possibly produced during reheating at a comfortably large reheat temperature of $T_{RH} \approx 10^{10}\text{GeV}$. Very heavy stau decays can still account for all the (gravitino) dark matter as shown in Fig. 6, nevertheless models at smaller $\tan\beta \sim 10$ seem more economical in the context of dark matter generation.

V. LITHIUM AND LIGHT GRAVITINOS

In this section we identify SUSY parameter space which results in significant changes of the primordial ${}^6\text{Li}$ and ${}^7\text{Li}$ abundances, in cases when the gravitino is rather light $m_{\tilde{G}} \lesssim 10\text{GeV}$. Such an analysis has so far not been performed. Light gravitinos are a typical prediction of gauge-mediated SUSY breaking scenarios (GMSB),

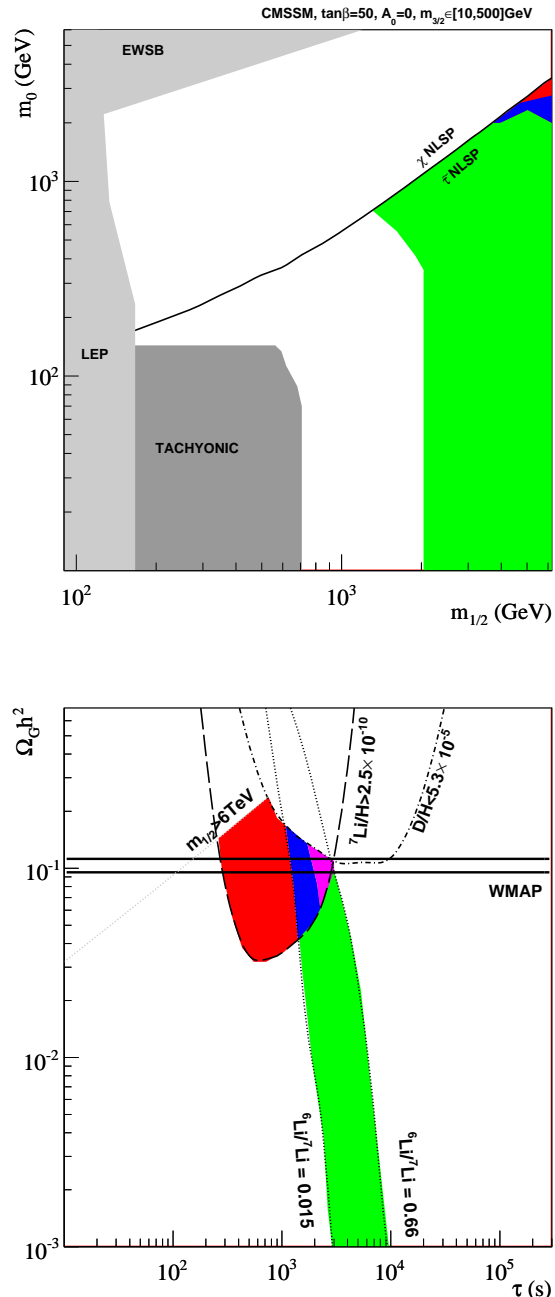


FIG. 6: Same as Figs.4 and 5, but for $\tan\beta = 50$. The region labeled "tachyonic" is excluded due to some sfermion masses becoming negative.

where SUSY breaking in a hidden sector is transmitted to the visible sector via gauge interactions of some messenger fields [78], [79]. Assuming a typical grand unified group, such models have three continuous and one discrete parameter, namely Λ , the common mass scale of the soft Susy breaking masses, M_{mess} , the Susy preserving messenger mass, $\tan\beta$, the ratio of the two higgs doublet vevs and N_{mess} the number of quark-like (as-

TABLE I: Light-element abundances yields and gravitino abundance $\Omega_{3/2}h^2$ for a number of selected models. Cf. to Table II for the particular particle model parameters. Model denoted by (a) have been computed with the invariant mass approximation (see text for details).

Model	D/H	${}^7\text{Li}/\text{H}$	${}^6\text{Li}/{}^7\text{Li}$	${}^9\text{Be}/\text{H}$	$\Omega_{3/2}h^2$
A	$3.45 \cdot 10^{-5}$	$2.20 \cdot 10^{-10}$	—	—	0.11
A ^a	$3.86 \cdot 10^{-5}$	$1.66 \cdot 10^{-10}$	—	—	0.11
B	$4.75 \cdot 10^{-5}$	$2.14 \cdot 10^{-10}$	0.058	$3.4 \cdot 10^{-14}$	0.10
B ^a	$5.42 \cdot 10^{-5}$	$1.83 \cdot 10^{-10}$	0.081	$3.8 \cdot 10^{-14}$	0.10
C ^a	$3.59 \cdot 10^{-5}$	$3.32 \cdot 10^{-10}$	0.044	$7.5 \cdot 10^{-14}$	0.0086
D ^a	$2.57 \cdot 10^{-5}$	$4.95 \cdot 10^{-10}$	0.044	$1.9 \cdot 10^{-13}$	$3 \cdot 10^{-4}$
E ^a	$3.61 \cdot 10^{-5}$	$2.09 \cdot 10^{-10}$	—	—	$2 \cdot 10^{-4}$

TABLE II: Particle physics model parameters corresponding to the abundance yields shown in Table I. All masses are in GeV and $\tan\beta = 10$

Model	SUSY - NLSP	M_{NLSP}	$m_{\tilde{G}}$	τ_X (s)
A	CMSSM $\tilde{\tau}$ ($m_0, m_{1/2}$) = (1045, 5020)	2060	160	403
B	CMSSM $\tilde{\tau}$ ($m_0, m_{1/2}$) = (678, 4200)	1638	175	1553
C	CMSSM $\tilde{\tau}$ ($m_0, m_{1/2}$) = (395, 1831)	763	30	1980
D	GMSB $N = 2 \tilde{\tau}$ (Λ, M_{mess}) = ($10^5, 5 \cdot 10^6$)	264	2.72	3320
E	GMSB $N = 1 \chi$ (Λ, M_{mess}) = ($10^5, 5 \cdot 10^6$)	133.8	0.08	103

sumed to be equal the number of lepton-like) multiplets (of some GUT group) messenger supermultiplets. The soft Susy breaking gaugino (square of scalar) masses are then generated at the 1- (2-) loop level, respectively, leading to the physical spectra and couplings of the MSSM particles. (The soft breaking trilinear couplings A are generated only at the two-loop level and will be set to zero). Even though the fine details of the MSSM spectrum and couplings depend on these four parameters, in most parts of the parameter space varying M_{mess} , which affects the soft masses only logarithmically, will be effectively irrelevant to our study. We are thus left with one free mass parameter Λ which should furthermore be of order 100 TeV if the MSSM spectrum is to remain at the electroweak mass scale. Such models are therefore more constrained than, for example, the CMSSM which has (at least) two mass parameters m_0 and $m_{1/2}$ (given that trilinear couplings A 's have been set to zero). Nevertheless, before discussing results in the GMSB, we will still study some aspects of the CMSSM when the gravitino

mass is (arbitrarily) low. Though not quite consistent, as one expects $m_{\tilde{G}} \sim m_{\text{soft}}$ when SUSY breaking in a hidden sector is communicated to the visible sector by gravitational interactions, the study of the CMSSM with light gravitinos may help to shed more light on existing "lithium-friendly" parameter space in models beyond the toy models CMSSM and GMSB.

Consulting Fig. 2 as the key figure of where to expect parameter space solving the ${}^7\text{Li}$ anomaly, one observes that for all $3 \times 10^{-4} \lesssim \Omega_{NLSP}h^2 B_h \lesssim 0.1$, and with a somewhat tuned gravitino mass to match the "desired" NLSP life time, solutions should exist. It is noted here that the exact range required in $\Omega_{NLSP}h^2 B_h$ depends on the NLSP mass M_{NLSP} , moving down as M_{NLSP} moves down (Fig. 2 assumes $M_{NLSP} = 1 \text{ TeV}$) and vice versa. As discussed above, stau NLSP abundances are not much larger than $\Omega_{\tilde{\tau}}h^2 \sim 1$ (cf. Eq. 6), whereas their hadronic branching ratios are usually small $B_h \lesssim 10^{-3}$. Thus, ${}^7\text{Li}$ solving areas for the stau maybe only found for large $m_{\tilde{\tau}} \sim 1 \text{ TeV}$ since only there $\Omega_{\tilde{\tau}}h^2 \sim 1$. Furthermore, to match the desired life time, large $m_{\tilde{\tau}}$ require large $m_{\tilde{G}}$ (cf. Eq. (2)), thus pointing towards gravity mediated susy breaking scenarios. These solutions have been all discussed in Section IV. In contrast, the freeze-out $\Omega_{\chi}h^2$ for neutralinos may be large $\sim 1 - 100$ and there hadronic branching ratio due to $\chi \rightarrow \tilde{G}q\bar{q}$ with an intermediate Z or photon is typically of the order of $B_h \sim 0.1$. In particular, one may find ${}^7\text{Li}$ -friendly models for comparatively light neutralinos only for which $\Omega_{\chi}h^2$ and B_h are not too large as to saturate the upper bound on $\Omega_{NLSP}B_h(NLSP)$ given by ${}^4\text{He}$ overproduction. Since τ_{χ} scales with m_{χ} to the fifth power, the gravitino mass $m_{\tilde{G}}$ in such decays has to be rather light in order to match the decay time window $100 \text{ sec} \lesssim \tau \lesssim 1000 \text{ sec}$ (cf. Fig. 2). Thus, one is automatically led to lighter gravitinos. This implies also, since Ω_{NLSP} may not be too large, and $\Omega_{3/2} = \Omega_{NLSP}(m_{\tilde{G}}/m_{NLSP})$ that only a small fraction of the dark matter would be created by such decays.

Identifying areas of small neutralino abundance in the CMSSM in the m_0 - $m_{1/2}$ plane, in order to satisfy $\Omega_{NLSP}B_h(NLSP) \lesssim 0.1$ (rather $\Omega_{NLSP}B_h(NLSP) \lesssim 0.03$ for $m_{\chi} \approx 100 \text{ GeV}$), is reminiscent of identifying the regions where $\Omega_{\chi} \sim \Omega_{WMAP}$ to account for neutralino dark matter. The latter question has received much attention over the last years. It is therefore not surprising that one finds potential ${}^7\text{Li}$ -solving parameter space in three distinct and "known" regions (a) the bulk region close to the LEP bound at small $m_{1/2} \approx 300 - 400 \text{ GeV}$, (b) the co-annihilation region close to the line of neutralino-stau mass degeneracy, and (c) the focus point region at large m_0 and $m_{1/2}$. These regions are shown in red in Fig. 7 for $\tan\beta = 10$. In contrast with the heavy gravitino case, here Higgs mass bounds from LEP could potentially exclude large fractions of the bulk region, as illustrated in the figure with lines of constant lightest Higgs mass including the Standard Model Higgs present lower limit $m_{H^0} \gtrsim 114 \text{ GeV}$. Although the experimental

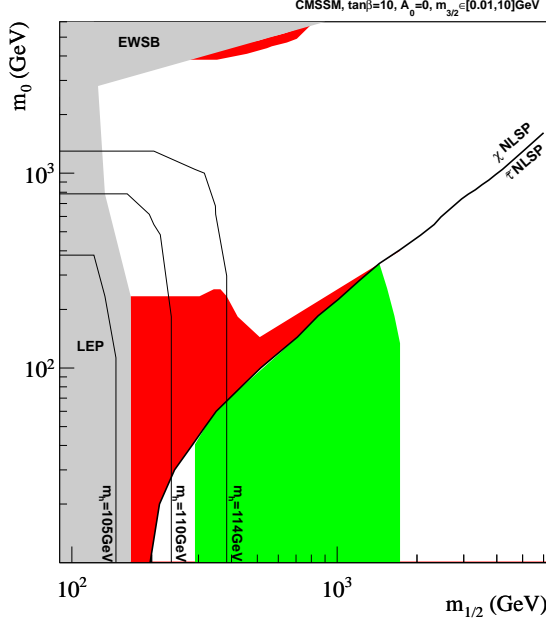


FIG. 7: ${}^7\text{Li}$ (red) and ${}^6\text{Li}$ (green) solving regions for a CMSSM model at $\tan\beta = 10$ and with light gravitinos in the range $10\text{ MeV} \lesssim m_{\tilde{G}} \lesssim 10\text{ GeV}$. All constraints and lines have similar meaning to those in Fig. 4. Note that the ${}^7\text{Li}$ solving regions exist essentially wherever $3 \times 10^{-4} \lesssim \Omega_{\text{NLSP}} h^2 B_h(\text{NLSP}) \lesssim 0.1$.

limits from LEP and Tevatron are milder for the MSSM higgses, one should keep in mind that a detailed study is needed, beyond the maximal mixing or no-mixing assumptions, in order to assess quantitatively the effect of experimental exclusions on our scenarios. There exists more parameter space to solve the ${}^7\text{Li}$ problem by neutralino decay than to produce neutralino dark matter of the right density (when $m_{\tilde{G}} > m_\chi$). Here region (a) requires gravitino masses $30\text{ MeV} \lesssim m_{\tilde{G}} \lesssim 100\text{ MeV}$, region (b) $200\text{ MeV} \lesssim m_{\tilde{G}} \lesssim 6.5\text{ GeV}$, whereas region (c) prefers $200\text{ MeV} \lesssim m_{\tilde{G}} \lesssim 800\text{ MeV}$. Note also that for larger $\tan\beta$ values ($\gtrsim 40$) a fourth ${}^7\text{Li}$ friendly funnel shaped region appears, corresponding to the well-known CP-odd higgs resonance effects.

We next study GMSB models. The blue sequence of points in Fig.2 shows the prediction for $\Omega_\chi h^2 B_h$ for NLSP neutralinos decaying into 100 MeV gravitinos in a particular GMSB model, employing $N_{\text{mess}} = 1$ (lepton- and quark-like) messenger particles of mass $M_{\text{mess}} = 5 \times 10^6\text{ GeV}$ and $\tan\beta = 10$. More accurate results for this model, now with varying $m_{\tilde{G}}$, are shown in Fig. 8. There clearly exists ${}^7\text{Li}$ -solving parameter space for light neutralinos $\lesssim 200\text{ GeV}$ detectable at the LHC. We have also shown in light blue the parameter space region consistent with standard BBN (whereas the white region is ruled out). This is interesting by itself, as it illustrates the overall consistency of GMSB scenarios with primor-

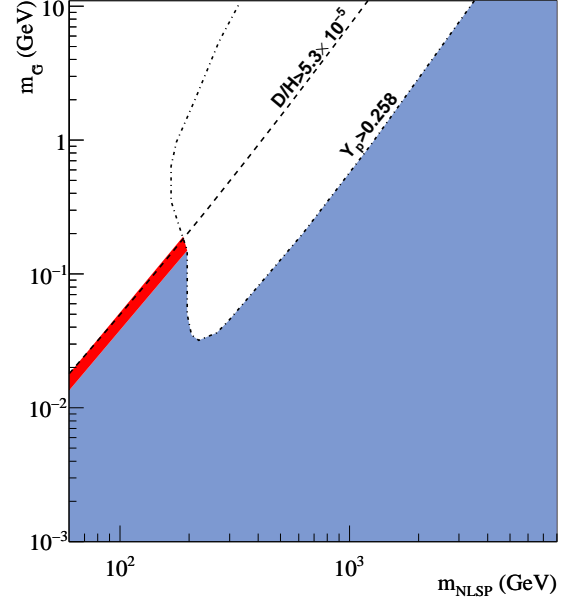


FIG. 8: Parameter space in the gravitino mass $m_{\tilde{G}}$ NLSP mass m_{NLSP} plane for light gravitinos $m_{\tilde{G}} < 10\text{ GeV}$ which significantly reduce the ${}^7\text{Li}$ abundance, i.e. ${}^7\text{Li}/\text{H} < 2.5 \times 10^{-10}$ (red), while respecting all other BBN constraints, as labeled. Here a GMSB model with $\tan\beta = 10$, $N_{\text{mess}} = 1$, and $M_{\text{mess}} = 5 \times 10^6\text{ GeV}$ has been assumed. Light-blue areas are allowed by BBN while white areas are ruled out.

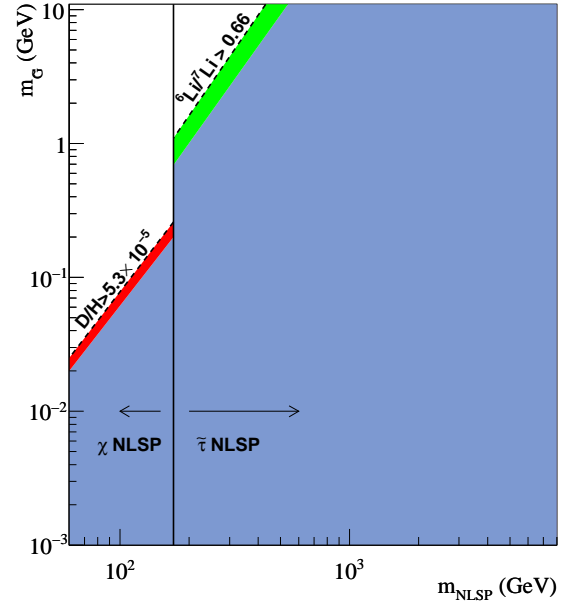


FIG. 9: As Fig. 8 but with $N_{\text{mess}} = 2$, leading to neutralino NLSPs for $m_{\text{NLSP}} \lesssim 175\text{ GeV}$ and stau NLSPs for $m_{\text{NLSP}} \gtrsim 175\text{ GeV}$ as indicated. The green area shows regions with $0.015 \lesssim {}^6\text{Li}/{}^7\text{Li} \lesssim 0.66$.

TABLE III: Potential for SUSY with gravitino LSPs to resolve the ${}^7\text{Li}$ problem, account for ${}^6\text{Li}$, produce ${}^9\text{Be}$, account completely for the dark matter due to non-thermal decay production, and be detectable at the LHC.

Gravitino	NLSP	${}^7\text{Li}$	${}^6\text{Li}$	${}^9\text{Be}$	$\Omega_{\text{DM}}h^2$	LHC
light	stau	X	\checkmark	$\checkmark?$	X	\checkmark
	neutralino	\checkmark	X	X	X	\checkmark
heavy	stau	\checkmark	\checkmark	$\checkmark?$	\checkmark	X
	neutralino	X	X	X	X	\checkmark

dial nucleosynthesis irrespective of whether the solution to the ${}^7\text{Li}$ problem is of particle physics or other astrophysical origin. In particular a combination of the standard bounds on ${}^4\text{He}$ mass fraction and Deuterium abundance cuts all gravitino masses $\gtrsim 200\text{ MeV}$ for a neutralino NLSP in the "natural" range $\lesssim 1\text{ TeV}$, thus reinforcing the common lore of light gravitinos within GMSB. Finally, we illustrate in Fig. 9 a GMSB scenario with two messenger (super)multiplets, $N_{\text{mess}} = 2$. In this case, the NLSP can be a stau or a neutralino, depending on the values of Λ . Here a ${}^6\text{Li}$ -solving pattern requires a stau NLSP heavier than $\sim 175\text{ GeV}$ with $m_{\tilde{G}} \gtrsim 1\text{ GeV}$, while solutions for ${}^7\text{Li}$ still obtain for a neutralino NLSP in the same part of the parameter space as in the $N_{\text{mess}} = 1$ case. The discontinuity in Fig. 9 is obviously due to the different nature of the NLSP, different hadronic branching ratios as well as absence of catalysis effects for neutralino NLSP. We note also that an intermediate range of gravitino masses is disfavoured if one insists on solving at least one of the two lithium problems on top of the consistency with standard BBN. However this gap in the mass range is obtained for a fixed messenger mass. We checked that it can be easily filled by varying the latter over a few orders of magnitude. Other patterns can appear by varying the number of messengers, or by relaxing the grand unification assumptions taking different numbers of quark-like and lepton-like messenger fields.

VI. CONCLUSIONS

The present paper has studied a variety of supersymmetric scenarios with gravitino LSPs. It has been mostly motivated by an apparent mismatch between the by standard BBN (SBBN) predicted ${}^7\text{Li}/\text{H}$ ratio and that observed in low-metallicity halo stars, as well as the (potentially controversial) claims of an observed ${}^6\text{Li}/{}^7\text{Li}$ plateau at low metallicity reminiscent of a ${}^6\text{Li}$ primordial abundance factor $\sim 10^3$ larger than predicted by SBBN. Though one or both of these anomalies may have an astrophysical/observational origin, it is conceivable

that they point to physics beyond the standard model of particle physics and BBN. In particular, supersymmetric (NLSP) particle decays during BBN may explain either one or both of these anomalies. Though not the first such study, the present study improves in accuracy on several accounts, as well as studies, for the first time, the case of light gravitinos $10\text{ MeV} \lesssim m_{\tilde{G}} \lesssim 10\text{ GeV}$. Detailed and improved analyses of relic NLSP abundances and hadronic branching ratios are performed in two distinct SUSY models, the CMSSM with heavy gravitinos $m_{\tilde{G}} \gtrsim 10\text{ GeV}$ (Section IV) and the GMSB with light gravitinos $m_{\tilde{G}} \lesssim 10\text{ GeV}$ (Section V). Other significant improvements concern the study of BBN yields due to NLSP hadronic decays when no simplifying assumptions are made about the injected nucleon spectrum (Section II), as well as the full inclusion of catalytic effects during BBN due to the presence of weak-mass scale electrically charged particles (i.e. the stau). Finally, approximate "model builders instructions" of where, on general grounds, to find relic particle decay parameter space relevant to the ${}^7\text{Li}$ and ${}^6\text{Li}$ abundances are given as well (Section III).

The general results of this study are summarized in Table III. Susy with either heavy or light gravitino LSPs may impact the cosmic lithium abundances while satisfying all other BBN constraints. Scenarios with heavy gravitinos require the charged stau to be the NLSP, and may solve the ${}^7\text{Li}$ problem with or without production of ${}^6\text{Li}$ in abundance as claimed to be observed in low-metallicity stars, while producing all the dark matter as inferred by WMAP. These conclusions are unchanged from earlier ones, independent of catalysis effects and improvements in hadronic branching ratios and injected nucleon spectrum due to the decay. However, in those parts of the parameter space where significant ${}^6\text{Li}$ is synthesized, interestingly, it is conceivable that ${}^9\text{Be}$ on levels consistent with observations is produced due to catalytic effects as well. Unfortunately, scenarios of stau NLSP with a heavy gravitino LSP are most likely untestable at the LHC, since $m_{\tilde{\tau}} \gtrsim 1\text{ TeV}$ is preferred. This is different for scenarios with light gravitinos. Here, either cosmologically important abundances of ${}^6\text{Li}$ (and possibly ${}^9\text{Be}$) may be synthesized (for stau NLSP) or the ${}^7\text{Li}$ problem may be solved (for neutralino NLSP) for NLSPs light enough to be detectable at the LHC. However, in such scenarios only a small fraction of the dark matter is produced, with the remaining gravitino dark matter possibly produced during a reheating period after inflation.

The authors acknowledge useful discussions with Asimina Arvanitaki, Savas Dimopoulos, Peter Graham, Lawrence Hall, Masayasu Kamimura, John March-Russell, Maxim Pospelov, and Frank Steffen. This work was supported in part by ANR under contract NT05-1.43598/ANR-05-BLAN-0193-03.

-
- [1] J. L. Feng, A. Rajaraman, and F. Takayama, Phys. Rev. Lett. **91**, 011302 (2003), hep-ph/0302215.
- [2] J. L. Feng, A. Rajaraman, and F. Takayama, Phys. Rev. D **68**, 063504 (2003), hep-ph/0306024.
- [3] J. R. Ellis, K. A. Olive, Y. Santoso, and V. C. Spanos, Phys. Lett. **B588**, 7 (2004), hep-ph/0312262.
- [4] J. L. Feng, S. Su, and F. Takayama, Phys. Rev. D **70**, 063514 (2004), hep-ph/0404198; J. L. Feng, S. Su, and F. Takayama, Phys. Rev. D **70**, 075019 (2004), hep-ph/0404231.
- [5] L. Roszkowski, R. Ruiz de Austri, and K.-Y. Choi, JHEP **08**, 080 (2005), hep-ph/0408227.
- [6] E. A. Baltz and H. Murayama, JHEP **05**, 067 (2003), astro-ph/0108172.
- [7] M. Fujii and T. Yanagida, Phys. Lett. **B549**, 273 (2002), hep-ph/0208191.
- [8] M. Lemoine, G. Moulataka, and K. Jedamzik, Phys. Lett. **B645**, 222 (2007), hep-ph/0504021.
- [9] K. Jedamzik, M. Lemoine, and G. Moulataka, Phys. Rev. D **73**, 043514 (2006), hep-ph/0506129.
- [10] D. G. Cerdeno, K.-Y. Choi, K. Jedamzik, L. Roszkowski, and R. Ruiz de Austri, JCAP **0606**, 005 (2006), hep-ph/0509275.
- [11] W. Buchmuller, L. Covi, J. Kersten, and K. Schmidt-Hoberg, JCAP **0611**, 007 (2006), hep-ph/0609142.
- [12] F. D. Steffen, JCAP **0609**, 001 (2006), hep-ph/0605306.
- [13] M. Kawasaki, K. Kohri, and T. Moroi, Phys. Lett. **B649**, 436 (2007), hep-ph/0703122.
- [14] J. Pradler and F. D. Steffen, Phys. Lett. **B666**, 181 (2008), 0710.2213.
- [15] J. Kersten and K. Schmidt-Hoberg, JCAP **0801**, 011 (2008), 0710.4528.
- [16] M. Kawasaki, K. Kohri, T. Moroi, and A. Yotsuyanagi, (2008), 0804.3745.
- [17] Eq.(1) is a simplified form which encompasses the various NLSP types and 2-body decays, such as stau NLSP decaying into $\tau\tilde{G}$, neutralino NLSP decaying into $\gamma\tilde{G}$, or into $Z\tilde{G}$. For instance, in the limit of pure bino-like neutralino and neglecting for simplicity the masses of all decay products except for the gravitino, the three cases above correspond to (κ, n) taking respectively the values (1,4), $(\simeq \rho \cos^2\theta_W, 3)$ and $(\simeq \rho \sin^2\theta_W, 4)$ where $\rho = (1 + 3(m_{\tilde{G}}^2/M_{\text{NLSP}}^2))$ and θ_W is the weak angle. We do not include here the higgs final state channel of the neutralino decays which is suppressed due to the almost pure bino content of the latter. The analyses presented in this paper rely however on the exact expressions for the lifetimes without any approximation.
- [18] WMAP, G. Hinshaw *et al.*, (2008), 0803.0732.
- [19] J. A. Thorburn, Astrophys. J. **421**, 318 (1994).
- [20] S. G. Ryan, J. E. Norris, and T. C. Beers, Astrophys. J. **523**, 654 (1999), astro-ph/9903059.
- [21] C. Charbonnel and F. Primas, (2005), astro-ph/0505247.
- [22] M. Asplund, D. L. Lambert, P. E. Nissen, F. Primas, and V. V. Smith, Astrophys. J. **644**, 229 (2006), astro-ph/0510636.
- [23] A. Hosford, S. G. Ryan, A. E. G. Perez, J. E. Norris, and K. A. Olive, (2008), 0811.2506.
- [24] P. Bonifacio and P. Molaro, Mon. Not. Roy. Astron. Soc. **285**, 847 (1997), astro-ph/9611043.
- [25] P. Bonifacio *et al.*, (2002), astro-ph/0204332.
- [26] J. Melendez and I. Ramirez, Astrophys. J. **615**, L33 (2004), astro-ph/0409383.
- [27] R. H. Cyburt, B. D. Fields, and K. A. Olive, (2008), 0808.2818.
- [28] B. S. Nara Singh, M. Hass, Y. Nir-El, and G. Haquin, Phys. Rev. Lett. **93**, 262503 (2004), nucl-ex/0407017.
- [29] G. Gyurky *et al.*, Phys. Rev. **C75**, 035805 (2007), nucl-ex/0702003.
- [30] LUNA, F. Confortola *et al.*, Phys. Rev. **C75**, 065803 (2007), 0705.2151.
- [31] T. A. D. Brown *et al.*, Phys. Rev. **C76**, 055801 (2007), 0710.1279.
- [32] A. Coc, E. Vangioni-Flam, P. Descouvemont, A. Adah-chour, and C. Angulo, Astrophys. J. **600**, 544 (2004), astro-ph/0309480.
- [33] S. Theado and S. Vauclair, Astron. and Astrophys. **375**, 70 (2001), astro-ph/0106080; M. Salaris and A. Weiss, Astron. and Astrophys. **376**, 955 (2001), astro-ph/0104406; M. H. Pinsonneault, G. Steigman, T. P. Walker, and V. K. Narayanan, Astrophys. J. **574**, 398 (2002), astro-ph/0105439; A. M. Boesgaard, A. Stephens, and C. P. Deliyannis, Astrophys. J. **633**, 398 (2005), astro-ph/0507625.
- [34] D. L. Lambert, AIP Conf. Proc. **743**, 206 (2005), astro-ph/0410418.
- [35] S. Vauclair and C. Charbonnel, Astrophys. J. **502**, 372 (1998), astro-ph/9802315.
- [36] O. Richard, G. Michaud, and J. Richer, Astrophys. J. **619**, 538 (2005), astro-ph/0409672.
- [37] A. Korn *et al.*, Nature **442**, 657 (2006), astro-ph/0608201.
- [38] K. M. Nollett, M. Lemoine, and D. N. Schramm, Phys. Rev. **C56**, 1144 (1997), astro-ph/9612197.
- [39] V. V. Smith, D. L. Lambert, and P. E. Nissen, Astrophys. J. **408**, 262S (1993); L. M. Hobbs and J. A. Thorburn, Astrophys. J. **491**, 772 (1997); V. V. Smith, D. L. Lambert, and P. E. Nissen, Astrophys. J. **506**, 405 (1998); R. Cayrel *et al.*, Astron. and Astrophys. **343**, 923 (1999), 9901205.
- [40] R. Cayrel *et al.*, (2007), 0708.3819; R. Cayrel, M. Steffen, P. Bonifacio, H.-G. Ludwig, and E. Caffau, (2008), 0810.4290.
- [41] N. Prantzos, (2005), astro-ph/0510122.
- [42] E. Rollinde, E. Vangioni, and K. A. Olive, Astrophys. J. **651**, 658 (2006), astro-ph/0605633.
- [43] B. B. Nath, P. Madau, and J. Silk, Mon. Not. Roy. Astron. Soc. Lett. **366**, L35 (2006), astro-ph/0511631.
- [44] V. Tatischeff and J. P. Thibaud, Astron. and Astrophys. **469**, 265 (2007), astro-ph/0610756.
- [45] S. Dimopoulos, R. Esmailzadeh, L. J. Hall, and G. D. Starkman, Astrophys. J. **330**, 545 (1988).
- [46] K. Jedamzik, Phys. Rev. Lett. **84**, 3248 (2000), astro-ph/9909445.
- [47] K. Jedamzik, Phys. Rev. **D70**, 063524 (2004), astro-ph/0402344.
- [48] M. Kawasaki, K. Kohri, and T. Moroi, Phys. Lett. **B625**, 7 (2005), astro-ph/0402490.
- [49] K. Jedamzik, Phys. Rev. **D70**, 083510 (2004), astro-ph/0405583.
- [50] DAMA, R. Bernabei *et al.*, (2008), 0804.2741.
- [51] J. R. Ellis, K. A. Olive, and E. Vangioni, Phys. Lett.

- B619**, 30 (2005), astro-ph/0503023.
- [52] K. Jedamzik, K.-Y. Choi, L. Roszkowski, and R. Ruiz de Austri, *JCAP* **0607**, 007 (2006), hep-ph/0512044.
 - [53] R. H. Cyburt, J. R. Ellis, B. D. Fields, K. A. Olive, and V. C. Spanos, *JCAP* **0611**, 014 (2006), astro-ph/0608562.
 - [54] K. Kohri and Y. Santoso, (2008), 0811.1119.
 - [55] D. Cumberbatch *et al.*, *Phys. Rev.* **D76**, 123005 (2007), 0708.0095.
 - [56] M. Pospelov, *Phys. Rev. Lett.* **98**, 231301 (2007), hep-ph/0605215.
 - [57] K. Kohri and F. Takayama, *Phys. Rev.* **D76**, 063507 (2007), hep-ph/0605243.
 - [58] M. Kaplinghat and A. Rajaraman, *Phys. Rev.* **D74**, 103004 (2006), astro-ph/0606209.
 - [59] K. Hamaguchi, T. Hatsuda, M. Kamimura, Y. Kino, and T. T. Yanagida, *Phys. Lett.* **B650**, 268 (2007), hep-ph/0702274.
 - [60] C. Bird, K. Koopmans, and M. Pospelov, (2007), hep-ph/0703096.
 - [61] K. Jedamzik, *Phys. Rev.* **D77**, 063524 (2008), 0707.2070.
 - [62] T. Jittoh *et al.*, *Phys. Rev.* **D76**, 125023 (2007), 0704.2914.
 - [63] M. Kusakabe, T. Kajino, R. N. Boyd, T. Yoshida, and G. J. Mathews, *Phys. Rev.* **D76**, 121302 (2007), 0711.3854.
 - [64] M. Pospelov, (2007), 0712.0647.
 - [65] M. Pospelov, J. Pradler, and F. D. Steffen, (2008), 0807.4287.
 - [66] M. Kamimura, Y. Kino, and E. Hiyama, (2008), 0809.4772.
 - [67] K. Jedamzik, *Phys. Rev. D* **74**, 103509 (2006), hep-ph/0604251.
 - [68] A. Djouadi, J.-L. Kneur, and G. Moultaka, *Comput. Phys. Commun.* **176**, 426 (2007), hep-ph/0211331.
 - [69] G. Belanger, F. Boudjema, A. Pukhov, and A. Semenov, *Comput. Phys. Commun.* **176**, 367 (2007), hep-ph/0607059.
 - [70] A. Pukhov, (2004), hep-ph/0412191.
 - [71] T. Sjostrand, S. Mrenna, and P. Skands, *JHEP* **05**, 026 (2006), hep-ph/0603175.
 - [72] Note that whereas catalytic effects are mostly dependent on $Y_X = n_X/n_B$ the X-particle-to-baryon ratio, hadronic effects are mostly dependent on $\Omega_X h^2 B_h \sim Y_X M_X B_h$, making it unpractical to show results dependent on either $\Omega_X h^2 B_h$ or Y_X .
 - [73] F. Primas, M. Asplund, P. E. Nissen, and V. Hill, (2000), astro-ph/0009482; A. M. Boesgaard and M. C. Novicki, *Astrophys. J.* **633**, L125 (2005), astro-ph/0509483; A. M. Boesgaard and M. C. Novicki, *Astrophys. J.* **641**, 1122 (2006), astro-ph/0512317.
 - [74] R. H. Cyburt, J. R. Ellis, B. D. Fields, and K. A. Olive, *Phys. Rev.* **D67**, 103521 (2003), astro-ph/0211258.
 - [75] T. Asaka, K. Hamaguchi, and K. Suzuki, *Phys. Lett.* **B490**, 136 (2000), hep-ph/0005136.
 - [76] M. Ratz, K. Schmidt-Hoberg, and M. W. Winkler, (2008), 0808.0829.
 - [77] J. Pradler and F. D. Steffen, (2008), 0808.2462.
 - [78] P. Fayet, *Phys. Lett.* **B78**, 417 (1978); M. Dine, W. Fischler, and M. Srednicki, *Nucl. Phys.* **B189**, 575 (1981); S. Dimopoulos and S. Raby, *Nucl. Phys.* **B192**, 353 (1981); M. Dine and W. Fischler, *Phys. Lett.* **B110**, 227 (1982); M. Dine and M. Srednicki, *Nucl. Phys.* **B202**, 238 (1982); M. Dine and W. Fischler, *Nucl. Phys.* **B204**, 346 (1982); L. Alvarez-Gaume, M. Claudson, and M. B. Wise, *Nucl. Phys.* **B207**, 96 (1982); C. R. Nappi and B. A. Ovrut, *Phys. Lett.* **B113**, 175 (1982); S. Dimopoulos and S. Raby, *Nucl. Phys.* **B219**, 479 (1983).
 - [79] M. Dine and A. E. Nelson, *Phys. Rev.* **D48**, 1277 (1993), hep-ph/9303230; M. Dine, A. E. Nelson, and Y. Shirman, *Phys. Rev.* **D51**, 1362 (1995), hep-ph/9408384; M. Dine, A. E. Nelson, Y. Nir, and Y. Shirman, *Phys. Rev.* **D53**, 2658 (1996), hep-ph/9507378.